



Urine macrophages reflect kidney macrophage content during acute tubular interstitial and glomerular injury

Ping-ping Sun^{a,e,f}, Xu-jie Zhou^{a,b,e,f}, Jian-qun Su^c, Chen Wang^{a,e,f}, Xiao-juan Yu^{a,b,e,f}, Tao Su^{a,e,f}, Gang Liu^{a,b,e,f}, Su-xia Wang^{a,b,d,e,f}, Jing Nie^{c,**}, Li Yang^{a,b,e,f,*}

^a Renal Division, Peking University First Hospital, Peking University Institute of Nephrology, Beijing, 100034, People's Republic of China

^b Renal Pathology Center, Peking University Institute of Nephrology, Beijing, 100034, People's Republic of China

^c State Key Laboratory of Organ Failure Research, National Clinical Research Center of Kidney Disease, Division of Nephrology, Nanfang Hospital, Southern Medical University, Guangzhou, 510515, People's Republic of China

^d Laboratory of Electron Microscopy, Pathological Center, Peking University First Hospital, Beijing 100034, People's Republic of China

^e Key Laboratory of Renal Disease, Ministry of Health of China, People's Republic of China

^f Key Laboratory of Chronic Kidney Disease Prevention and Treatment (Peking University), Ministry of Education, People's Republic of China

ARTICLE INFO

Keywords:

Acute kidney injury
Biomarker
Diagnosis
Macrophage
sCD163

ABSTRACT

Macrophage polarization is a major contributing factor in acute kidney injury (AKI). We aim to determine its biomarker value in differentiating etiologic causes of various intrinsic renal AKI. A total of 205 patients with renal intrinsic AKI were enrolled. Urinary sCD163 was quantified and macrophage subtypes in urine and in renal biopsy were determined. Compared to healthy controls and AKI due to interstitial or tubular injuries (0 pg/ μmol), urinary sCD163 was markedly higher in glomerulopathy, especially in diffuse proliferative glomerulonephritis (275.5 pg/ μmol) and significantly correlated with cellular crescent formation. Urine sediment analysis of M1/M2 ratio could differentiate acute tubulointerstitial nephritis (M1/M2 > 2.35) from crescentic glomerulonephritis (M1/M2 < 0.27). Urinary sCD163 levels and M2 subtype positively correlated with infiltrated M2 in the glomeruli, whereas urine M1 positively correlated with infiltrated M1 in the interstitium. Of note, urinary sCD163 showed better diagnostic performance in differentiating disease etiologies compared to traditional urinary biomarkers of AKI (NGAL and KIM-1) and markers of myeloid cells (CD11b) and pan macrophages (CD68). Thus markers of macrophage polarization could be viewed as the noninvasive “liquid biopsy” in the presence of various intrinsic kidney diseases.

1. Introduction

Acute kidney injury (AKI) is a common disorder characterized by an acute decline in renal function and is associated with increased mortality rate, hospitalization time, and total health-related costs [1–4]. In recent years, several urinary biomarkers have become available for early detection of AKI [5–12], such as urinary cystatin C, urinary kidney injury molecule 1 (KIM-1), and urinary/plasma neutrophil gelatinase-

associated lipocalin (NGAL). But in most biomarker studies, proof of the specificity of biomarker changes for diagnosing the location of the injury and identifying various changes in renal pathology has been lacking [1,12,13]. Additional biomarkers are needed to provide more detailed information about the type, intensity, and location of kidney tissue injury as the adoption of therapeutic interventions can be highly distinguished among different etiological causes of intrinsic renal AKI.

Increasing data demonstrate that macrophages are major

Abbreviations: AKI, acute kidney injury; AKD, acute kidney disease; ANCA, anti-neutrophil cytoplasmic antibodies; ATN, acute tubular necrosis; ATIN, acute tubulointerstitial nephritis; Cres-GN, crescentic glomerulonephritis; DN, diabetic nephropathy; DPGN, diffuse proliferative glomerulonephritis; ELISA, enzyme-linked immunosorbent assay; Endo-prolif.GN, endocapillary proliferative glomerulonephritis; FPGN, focal proliferative GN; KDIGO, the Kidney Disease: Improving Global Outcomes; MCD, minimal change disease; MN, membranous nephropathy; MPGN, membranoproliferative glomerulonephritis; PGN, proliferative glomerulonephritis; ROC, receiver–operator characteristic; sCD163, soluble CD163; TMA, thrombotic microangiopathy; KIM-1, kidney injury molecule 1; NGAL, neutrophil gelatinase-associated lipocalin

* Correspondence to: L. Yang, Renal Division, Peking University First Hospital, Peking University Institute of Nephrology; Key Laboratory of Chronic Kidney Disease Prevention and Treatment (Peking University), Ministry of Education, No. 8, Xishiku Street, Xicheng District, Beijing 100034, People's Republic of China.

** Corresponding author.

E-mail addresses: niejing@smu.edu.cn (J. Nie), li.yang@bjmu.edu.cn (L. Yang).

<https://doi.org/10.1016/j.clim.2019.06.005>

Received 13 February 2019; Received in revised form 3 May 2019

Available online 15 June 2019

1521-6616/© 2019 Elsevier Inc. All rights reserved.

contributors to the inflammatory response to AKI [9,14–18]. And Macrophages play a complex role throughout AKI by their functional plasticity between the pro-inflammatory (classically activated/M1) and pro-reparative (alternatively activated/M2) macrophages polarization. It is suggested that macrophage polarization may open the possibility for the identification of novel biomarkers and aid in the development of effective therapeutic targets [5,8,12,14,16,19]. Classical biological markers for M1 macrophages include MHC class II (HLA-DR), CD80/CD86 and IL-1R, and for biological markers for M2 macrophages include mannose receptor (CD204, CD206), scavenger receptor (CD163) and CD23 [15–17]. More recent data indicated that CD163+ M2 macrophages predominate in renal biopsies of proliferative glomerulonephritis including lupus nephritis, anti-neutrophil cytoplasmic antibodies (ANCA)-associated pauci-immune necrotizing GN and membranoproliferative glomerulonephritis, and urinary soluble CD163 (sCD163) level reflects glomerular inflammation in each disease condition [20–24]. A more recent report suggested that urinary CD11b, a marker for both neutrophils and macrophages, was superior to CD163 for the prediction of histopathological activity in proliferative lupus nephritis [25]. However, the utility of urinary sCD163 and other urine macrophage markers in differentiating various renal tissue injury has not been investigated.

To further explore macrophage polarization and address its biomarker role in human intrinsic renal AKI, we aim to determine the value of using urinary sCD163, urine sediment macrophage subtypes, and renal infiltrated macrophage subtypes/locations in differentiating etiologic causes of intrinsic renal AKI in a large cohort. The diagnostic performance was also compared to traditional markers of acute kidney injury (NGAL and KIM-1) and markers of myeloid cells (CD11b) and pan macrophages (CD68).

2. Materials and methods

2.1. Patients and samples

A total of 205 patients from Peking University First Hospital with acute kidney injury (AKI) and/or acute kidney disease (AKD) verified by renal biopsy from January 1st, 2012, to June 30th, 2016, were enrolled in the study. AKI and AKD were defined using the Kidney Disease: Improving Global Outcomes (KDIGO) criteria and consensus report of the Acute Disease Quality Initiative (ADQI) 16 Workgroup [26,27]. All the patients were grouped according to the main damage of the structures including tubules, interstitium, glomeruli, or intrarenal blood vessels. These included 11 patients with acute tubular necrosis (ATN), 24 patients with acute tubulointerstitial nephritis (ATIN), 4 patients with thrombotic microangiopathy (TMA), and 166 patients with proliferative glomerulonephritis (PGN), among which 124 cases were grouped into diffuse proliferative glomerulonephritis (DPGN) which included membranoproliferative glomerulonephritis (MPGN), endocapillary proliferative glomerulonephritis (Endo-prolif.GN), and crescentic glomerulonephritis (Cres-GN), and the other 42 patients were defined as focal proliferative GN (FPGN) due to various etiologies. Patient enrollment and the pathological diagnostic criteria can be referred to Supplementary Fig. 1 and Table 1. Thirty patients with non-proliferative glomerulopathy (non-P-GN) were randomly included as disease controls, including 5 patients with minimal change disease (MCD), 12 patients with membranous nephropathy (MN), and 13 patients with diabetic nephropathy (DN). Patients with acute inflammatory diseases such as fever, urinary tract infection, active liver diseases and sepsis were excluded. Clinical and laboratory data were collected from medical records at the time of renal biopsy.

Morning urine samples were collected on the day of renal biopsy, and urinary sCD163, CD68, CD11b, KIM-1 and NGAL were quantified. M1/M2 macrophage subtypes in urine sediments were randomly analyzed in 81 patients, and M1/M2 macrophage subtypes in renal biopsy specimens were examined. Morning urine samples from 19 healthy

Table 1

Pathologic diagnostic and inclusion criteria.

Pathological types of intrinsic AKI	
Proliferative glomerulonephritis (PGN)	Any of various types of glomerulonephritis characterized by increased glomerular cellularity caused by indigenous cells and/or leukocyte infiltration, including histological patterns as mesangial proliferative, endocapillary proliferative, membranoproliferative, necrotizing, and crescentic glomerulonephritis (GN).
Focal (FPGN):	Involving < 50% of glomeruli.
Diffuse (DPGN):	Involving ≥50% of glomeruli.
Crescentic glomerulonephritis (Cres-GN)	At least 50% of non-sclerosing glomeruli showing crescents, with severe damage of glomerular capillary loops in lesions.
Membranoproliferative glomerulonephritis (MPGN)	Diffuse proliferation of mesangial cell and matrix, mesangial interposition and glomerular basement membrane (GBM) thickening with double contours, deposition of immune complex in mesangial and subendothelial areas.
Endocapillary proliferative glomerulonephritis (Endo-prolif. GN)	Increased cellularity internal to the GBM composed of leukocytes, endothelial cells, and/or mesangial cells, with occlusion of capillary loops.
Acute tubular necrosis (ATN)	Renal tubular epithelia showing loss of the apical brush border with simplification and thinning of epithelia, coagulation necrosis with denuded tubular basement membrane, tubular lumen dilation with cellular debris and casts formation, focal tubular cell regeneration, along with interstitial edema and sparsely inflammatory cell infiltration.
Acute tubulointerstitial nephritis (ATIN)	Patchy or diffuse interstitial infiltration of inflammatory cells including lymphocytes, mononuclear cells and eosinophils, along with different degree of tubular injury.
Thrombotic microangiopathy (TMA)	Thrombosis of glomerular capillaries, diffuse proliferation and swelling of glomerular endothelial cells with occluded capillary lumens, thickened GBM with segmental double contour, focal mesangiolysis with microaneurism. Arterioles showing intimal mucoid edema and onion-skin change with narrowed lumens, occasionally with vascular thrombosis.

volunteers as healthy controls were also collected with the same procedures.

The protocol concerning the use of patient samples in this study was approved by the Institutional Review Board of Peking University First Hospital. Informed consent was obtained from all participants.

2.2. Measurement of urinary sCD163, CD68, CD11b, KIM-1 and NGAL in urine samples

Urinary (u-) sCD163 (RAB0082-1KT, Sigma), CD68 (CSB-E15979h, CUSABIO), CD11b (CSB-E11638h, CUSABIO), KIM-1 (DKM100, R&D) and NGAL (ab215541, Abcam) concentrations were measured using enzyme-linked immunosorbent assay (ELISA) kits according to the manufacturer's instructions. The levels of these markers were normalized to the urinary creatinine level before analysis.

2.3. Renal histology

Standard processing of kidney biopsy specimens included light microscopic (hematoxylin and eosin, periodic acid-Schiff, Masson's trichrome staining, and Jones methenamine silver), immunofluorescence and electronic microscopic examinations. The presence of glomerular lesions, including crescents and glomerulosclerosis, was calculated as the percentage relative to the nonsclerosis and the total number of glomeruli in a biopsy respectively. Tubular and interstitial lesions were scored semiquantitatively on the basis of the percentage of the tubulointerstitial compartment that was affected: loss of brush border, tubular atrophy, interstitial infiltrate and interstitial fibrosis (1 for 0–25%, 2 for 25–50%, 3 for 50–75% and 4 for > 75%).

2.4. Immunostaining of urine sediments for macrophage subtypes

Fresh urine sediments were resuspended with 300 µl PBS, and 30 µl

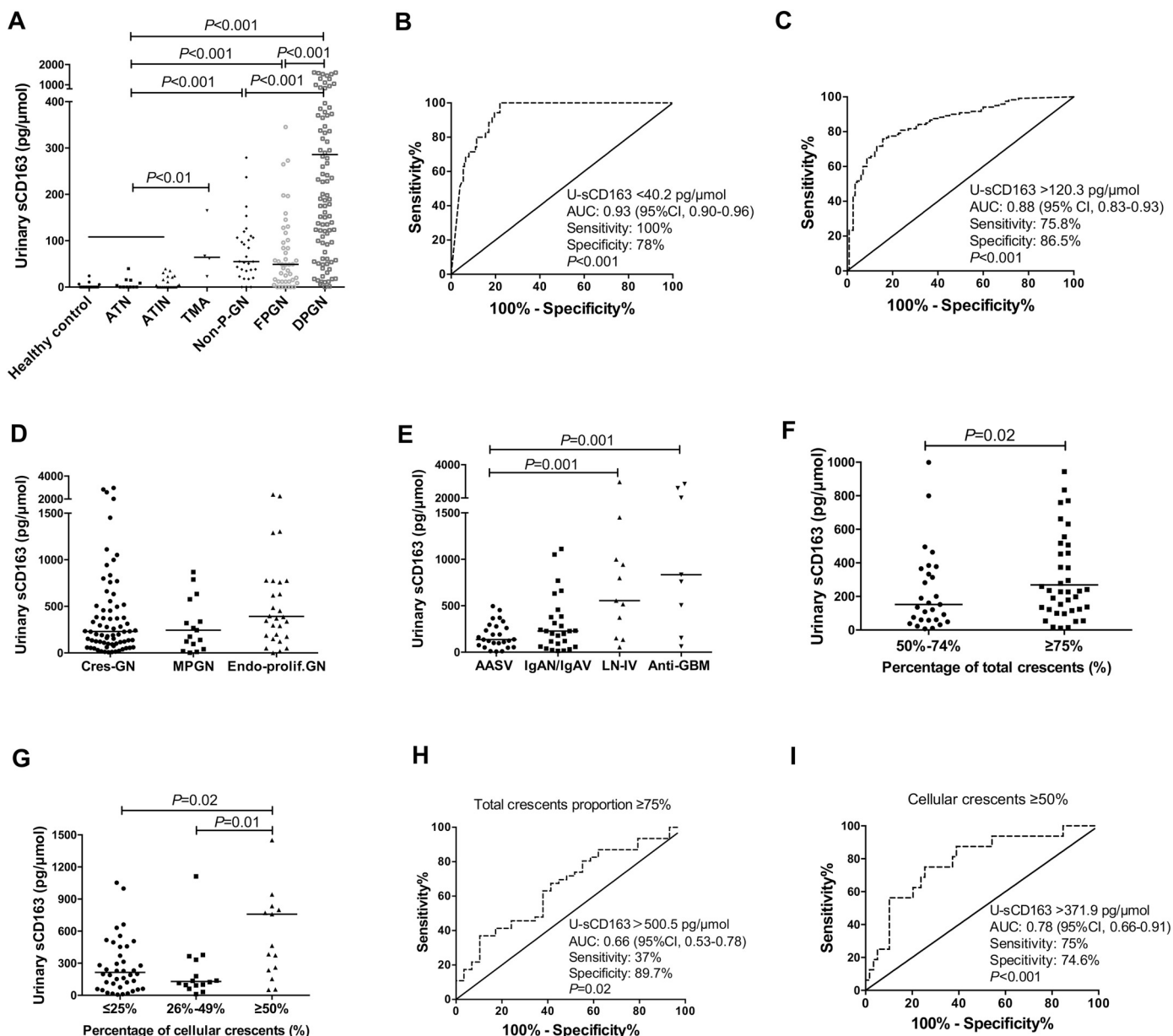


Fig. 1. U-sCD163 levels in different groups of patients and the diagnostic significance. (A) Comparison of u-sCD163 levels among different groups. (B–C) ROC curves derived from all the patients depicting the ability of u-sCD163 levels to detect ATIN/ATN (B) and DPGN (C). (D) Comparison of u-sCD163 levels among different groups of DPGN. (E) Comparison of u-sCD163 levels among patients with Cres-GN of different causes. (F) Comparison of u-sCD163 levels between Cres-GN patients with different percentage of total crescents formation. (G) Comparison of u-sCD163 levels among Cres-GN patients with different percentage of cellular crescents formation. (H–I) ROC curves derived from Cres-GN patients depicting the ability of u-sCD163 to detect total crescents percentage of $\geq 75\%$ (H) and cellular crescents percentage of $\geq 50\%$ (I). Values are presented as median; $P < .05$ was considered statistically significant.

of the resuspended urine sediments were swung on a glass slide by cytopsin centrifuges (Thermo Scientific, MA, USA). The slides were incubated with primary antibodies at 4 °C overnight. Mouse anti-human CD68 (1:500, ZM-0060; ZSGB-BIO) and rabbit anti-human HLA-DR (1:250, ab92511; Abcam) were used to recognize M1 macrophages, while mouse anti-human CD68 (1:500, ZM-0060; ZSGB-BIO) and rabbit anti-human CD163 (1:250, ab189915; Abcam) were used for M2 macrophages. Fluorescein secondary antibodies including donkey anti-mouse IgG AlexaFluor 488 (1:500, lot 125,268; Jackson ImmunoResearch) and donkey anti-rabbit IgG AlexaFluor 594 (1:500, lot 125,281; Jackson ImmunoResearch) were applied. Slides were then stained with 4'-6-diamidino-2-phenylindole (DAPI) (ZLI-9557; ZSGB-BIO) and mounted with a coverslip. Images were captured with the 90i microscope (Eclipse90i, Nikon, Tokyo, Japan). The average number of

macrophage subtypes in urine sediments was determined by examining at least 10 high power fields (400×) from each patient sample. NIS software (Nikon) was used to count cells, and M1/M2 was defined as the average number of M1 macrophages/average number of M2 macrophages in at least 10 high power fields.

2.5. Immunostaining of macrophage subtypes in renal biopsy samples

Immunofluorescence was performed on renal biopsy samples to detect macrophage subtypes. After deparaffinization and rehydration, antigen retrieval was performed by heating the slides in EDTA. The slides were incubated with primary and secondary antibodies the same as in urine sediments. Glomerular basement membrane (GBM) was stained with mouse anti-human $\alpha 3$ chain of type IV collagen (COL1V

(α3)) (1:50, AP0105; Euro Diagnostica AB). Images were captured with the 90i microscope (Nikon) or confocal microscope (LSM-780, Zeiss). Positive macrophage subtypes were analyzed at four compartments including glomerulus, interstitium, tubule wall and tubular lumen. The number of positive cells in glomeruli was expressed as the number of positive cells per glomerulus cross section. The number of positive cells in the interstitium, tubule wall and tubular lumen was expressed as the number of positive cells per high power field (400×). At least ten high power fields were analyzed, and results were expressed as the mean ± standard error (SEM).

2.6. Statistical analysis

Data were analyzed using SPSS version 19.0 (SPSS Inc., Chicago, IL, USA) and GraphPad Prism version 6 (GraphPad Software, San Diego, CA). Continuous data were presented as the mean ± SD or mean ± SEM, and the difference among groups was assessed using the *t*-test or one-way ANOVA. Nonnormally distributed data were presented as the median and interquartile range (IQR). Differences between two groups were analyzed using the Mann–Whitney *U* test, while differences between three or more groups using Kruskal–Wallis test with a post hoc Dunn's test. Assessment of the predictive capacity of urinary sCD163 and urinary macrophage subtypes in active renal inflammatory damage was based on the area (AUC) under the receiver–operator characteristic (ROC) curve, sensitivity, and specificity values. The point on the ROC curve that maximized the sum of sensitivity and specificity represented an optimal cutoff. Correlations were assessed according to the *Pearson* test for parametric data and the *Spearman* test for non-parametric data. A two-sided *P* < .05 was considered statistically significant.

3. Results

3.1. Urinary sCD163 levels are significantly elevated in diffuse proliferative GN

The detailed summary of the clinical and histopathological data from 205 patients with intrinsic acute renal injuries are shown in Supplementary Table 1.

Compared to healthy controls (0 pg/μmol, *n* = 19), there was no difference in the level of u-sCD163 in patients with ATN (0, 0–14.8 pg/μmol) or ATIN (0, 0–20 pg/μmol). However, u-sCD163 levels were significantly increased in patients with TMA or various glomerular diseases compared to either healthy controls or to ATN/ATIN (Fig. 1A). It was observed that the increase was milder in the conditions of TMA (64.3, 32.4–140.5 pg/μmol, *P* < .01), non-proliferative glomerulopathy (non-P-GN) such as MCD, MN, and DN (55.1, 31.7–107.4 pg/μmol, *P* < .001), and focal proliferative glomerulonephritis (FPGN) (48.8, 11.7–119.8 pg/μmol, *P* < .001), but the increase was much significantly profound in patients with diffuse glomerulonephritis (DPGN) (275.5, 121.1–631.7 pg/μmol, *P* < .001), which was 4–6 times higher compared to TMA, non-P-GN and FPGN (*P* < .001) (Supplementary Table 2).

ROC curves were adopted to examine the ability of u-sCD163 to differentiate pathological damage structures of intrinsic acute renal injuries in patients. The chosen cutoff < 40.2 pg/μmol diagnosed ATN/ATIN (i.e., AKI/AKD due to tubular/interstitial origin) with specificity of 78% and sensitivity of 100% (AUC 0.93, 95% CI 0.90–0.96, *P* < .001, Fig. 1B). The chosen cutoff > 120.3 pg/μmol diagnosed DPGN with specificity of 86.5% and sensitivity of 75.8% (AUC 0.88, 95% CI 0.83–0.93, *P* < .001, Fig. 1C).

3.2. Urinary sCD163 levels correlate with cellular crescents proportion in Cres-GN

We next determined whether the increase in u-sCD163 levels was

related to different glomerular pathological types and the underlying etiological causes. In DPGN, no significant differences were detected among pathological subgroups including MPGN (243.8, 68–604.6 pg/μmol), Endo-prolif.GN (379, 178–775 pg/μmol), and Cres-GN (232, 99–517 pg/μmol) (Fig. 1D). However, when the Cres-GN subgroup was further divided by underlying etiological causes, there was a significantly increased u-sCD163 tendency from AASV (136.2, 70.1–282.1 pg/μmol), IgAN/IgAV (227.7, 68.6–439.6 pg/μmol), LN (536.5, 207.3–985.2 pg/μmol), to anti-GBM disease (834.8, 329.4–2300.1 pg/μmol) (Fig. 1E).

A further correlation of urinary sCD163 with clinical and pathological parameters in Cres-GN was then conducted. It was evident that u-sCD163 levels positively correlated with serum creatinine levels both at peak (*r* = 0.39, *P* = .001) and at biopsy (*r* = 0.37, *P* = .001), proteinuria (*r* = 0.34, *P* = .01), and with the proportions of cellular crescents in renal pathology examination (*r* = 0.23; *P* = .04). When all the patients (*n* = 205) were grouped by the level of urinary sCD163 (high, median and low subgroup were defined according to interquartile range of urinary sCD163: ≤25%, 25%–75%, ≥75%), we observed that patients with higher levels of u-sCD163 showed higher levels of proteinuria (mean proteinuria, high vs. median vs. low: 5.2 vs. 4.0 vs. 1.0 g/d; *P* < .001), higher proportions of total crescents (57% vs. 40% vs. 0%; *P* < .001) and cellular crescents (13% vs. 7.7% vs. 0%; *P* < .001) (Table 2; Supplementary Tables 3 and 4). It indicated a relevance of u-sCD163 to the severity and activity of glomerular injury.

ROC curves for u-sCD163 were further developed to assess the ability of u-sCD163 in predicting the severity and activity of crescentic GN. AUC was 0.66 (95% CI 0.53–0.78, *P* = .02) for total crescents proportion ≥ 75% (Fig. 1H), and 0.78 (95% CI 0.66–0.91, *P* < .001) for cellular crescents proportion ≥ 50% with the chosen cut-off value of u-sCD163 > 371.9 pg/μmol (Fig. 1I). However, when correlation analysis between u-sCD163 and cellular crescents proportion was conducted in FPGN, MPGN and Endo-prolif.GN, no significant associations were observed (Table 2). These data suggest that elevated urinary sCD163 levels preferably indicate disease activity in crescentic GN.

3.3. Compared to KIM-1, NGAL, CD68 and CD11b, urinary sCD163 showed better fit in differentiating DPGN

We next observed urinary traditional AKI biomarkers (KIM-1, NGAL) and biomarkers for myeloid cells (CD11b) and pan macrophages (CD68) in our patients. It is interesting to note that urinary levels of KIM-1 and NGAL were significantly elevated in all the AKI groups compared to healthy controls, with patients of DPGN presenting the highest values among all the groups. Urinary CD11b level was also increased in all the AKI patients, with both ATIN and DPGN groups having comparable highest levels among different groups. Urinary level of CD68 was observed to be significantly elevated only in patients with DPGN but not in those of other AKI groups (Supplementary Table 2).

We then compared the diagnostic value of different urinary biomarkers and found that u-sCD163 was the best to differentiate ATN/ATIN (Fig. 2A; Supplementary Table 5). It showed that the AUC of u-sCD163 (cutoff: < 40.2 pg/μmol; sensitivity: 100%; specificity: 78%), u-CD68 (cutoff: < 0.83 pg/μmol; sensitivity: 61%; specificity: 75%), u-CD11b (cutoff: > 12.5 ng/μmol; sensitivity: 50%; specificity: 71.5%), u-KIM-1 (cutoff: < 0.86 ng/μmol; sensitivity: 41%; specificity: 94%), u-NGAL (cutoff: > 62.8 ng/μmol; sensitivity: 69%; specificity: 57.5%), was 0.93, 0.68, and 0.55, 0.71, 0.60 in the differentiation of ATIN/ATN. In addition, the area under the curve of u-sCD163 was also superior to those of u-CD11b and u-CD68 for predicting DPGN (Fig. 2B; Supplementary Table 5). The AUC of urine sCD163 (cutoff: > 120.3 pg/μmol; sensitivity: 75.8%; specificity: 86.5%), CD68 (cutoff: > 0.92 pg/μmol; sensitivity: 66%; specificity: 69%), and CD11b (cutoff: > 4.35 ng/μmol; sensitivity: 71.4%; specificity: 66.7%) and u-KIM-1 (cutoff: > 0.43 ng/μmol; sensitivity: 73%; specificity: 67.7%), u-NGAL (cutoff: > 11.9 ng/μmol; sensitivity: 91%; specificity: 39.4%), was 0.88, 0.72, and 0.72,

Table 2
Correlation of urinary sCD163 with renal function and clinicopathological parameters in patients with PGN.

	u-sCD163 in FPGN		u-sCD163 in DPGN			
			Non-Cres-DPGN		Cres-GN	
	(n = 42)		(n = 49)		(n = 75)	
	r	P	r	P	r	P
Serum creatinine (mg/dl)						
At peak	0.22	0.16	0.001	0.99	0.39	0.001
At biopsy	0.15	0.35	−0.05	0.72	0.37	0.001
Pathological changes						
Glomerular						
Total crescents (%)	−0.09	0.57	0.12	0.43	0.24	0.04
Cellular	−0.17	0.28	0.24	0.10	0.23	0.04
Cell-fibrous	−0.22	0.16	−0.002	0.99	−0.09	0.47
Fibrous	0.15	0.34	−0.16	0.26	−0.15	0.21
Sclerosis (%)	−0.12	0.43	−0.19	0.20	−0.04	0.74
Tubular						
Brush border loss	0.22	0.16	0.23	0.11	−0.15	0.21
Atrophy	0.003	0.98	−0.16	0.29	0.01	0.94
Interstitial						
Inflammation	−0.09	0.57	−0.26	0.08	0.01	0.92
Inflammation	−0.008	0.96	−0.25	0.08	0.01	0.93
Fibrosis	−0.12	0.45	−0.24	0.10	0.01	0.92

Abbreviation: U-sCD163, urinary soluble CD163; PGN, proliferative glomerulonephritis; FPGN, focal proliferative glomerulonephritis; DPGN, diffuse proliferative glomerulonephritis; Non-Cres-DPGN, none crescentic diffuse proliferative glomerulonephritis; Cres-GN, crescentic glomerulonephritis. The bold meant elevated urinary sCD163 levels preferably indicate disease activity in crescentic GN.

0.77, 0.67 for DPGN. It also showed better performance (AUC for sCD163 was 0.86, 95% CI 0.81–0.90) than proteinuria (AUC: 0.62, 95% CI 0.53–0.70) in predicting DPGN (Fig. 2C). Combining these biomarkers slightly improved the diagnostic efficiency of u-CD163 for identifying ATN/ATIN, but did not improve its diagnostic efficiency for DPGN (Fig. 2; Supplementary Table 5).

3.4. Urine sediment macrophage subtypes help differentiate renal acute injuries

The urine sediment macrophage subtypes were examined in 81 patients along with u-sCD163 levels (Fig. 3A). Urinary total macrophage count was highest in patients with Cres-GN (median 11.2), middle in ATIN, FPGN and non-Cres-DPGN (median 6.9–8.2), and lowest in patients with ATN, TMA or non-proliferative glomerulopathy (median 0.48) (Fig. 3B, Supplementary Table 6). Although significant differences among different disease groups were observed (P < .001), it was still difficult to differentiate ATIN from PGN by total macrophage quantification.

Interestingly, urine sediment M1 macrophage quantification was highest in patients with ATIN, followed by those with FPGN, non-Cres-DPGN and Cres-GN (Fig. 3C). While M2 macrophage quantification had

an inverse tendency, with the lowest value detected in the ATIN group and increasing values in patients with FPGN, non-Cres-DPGN, and Cres-GN successively (Fig. 3D). Therefore, the ATIN group had the highest urine sediment M1/M2 ratio (3.6, 2.4–19.3) and Cres-GN group presented the lowest ratio (0.08, 0.02–0.26). It was remarkable that urine sediment M1/M2 ratio of ATIN was 45 times high as that of Cres-GN (Fig. 3E, Supplementary Table 6).

ROC curves were then generated to examine the ability of urine sediment macrophage subtype quantification in differentiating pathological causes of acute kidney injuries. The area under the ROC curve was 0.99 for ATIN (95% CI 0.96–1.01, P < .001, sensitivity 98%, specificity 100%) with a cut-off value of M1/M2 > 2.35 (Fig. 3F); 0.63 for DPGN (95% CI 0.66–0.92, P < .001, sensitivity 62%, specificity 92%) (Fig. 3G) and 0.82 for crescentic GN (95% CI 0.72–0.93, P < .001, sensitivity 100%, specificity 69%) with a cut-off value of M1/M2 < 0.27 (Fig. 3H).

3.5. Urine macrophage polarization markers associate with renal infiltrated macrophage subtypes

We next performed anti-CD68, anti-CD163, and anti-HLA-DR immunostainings on the renal biopsy specimens from these patients to

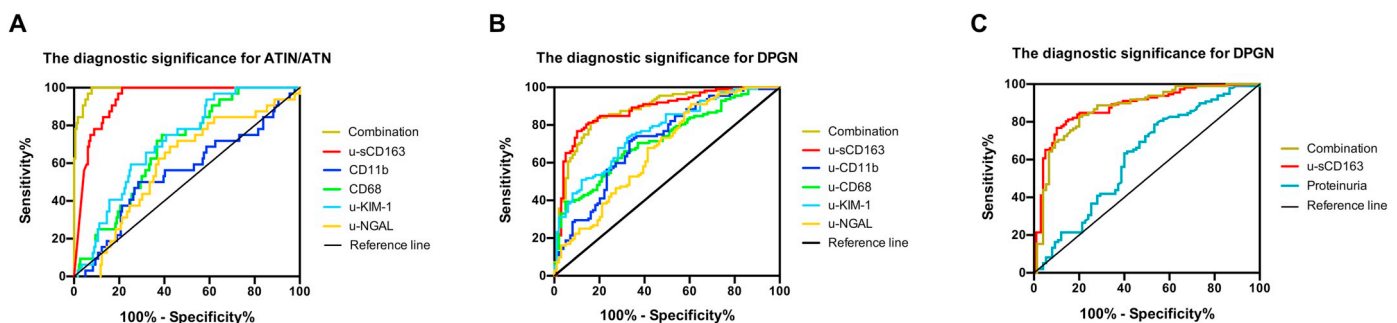


Fig. 2. Comparison the diagnostic significance of u-sCD163 and traditional AKI biomarkers (KIM-1 and NGAL) and other macrophage biomarkers (CD68 and CD11b). (A) ROC curves derived from all the patients depicting the ability of u-sCD163, u-CD11b, u-CD68, u-KIM-1 and u-NGAL levels to detect ATIN/ATN. (B) ROC curves derived from all the patients depicting the ability of u-sCD163, u-CD11b, u-CD68, u-KIM-1 and u-NGAL levels to detect DPGN. (C) ROC curves derived from all the patients depicting the ability of u-sCD163 and proteinuria levels to detect DPGN.

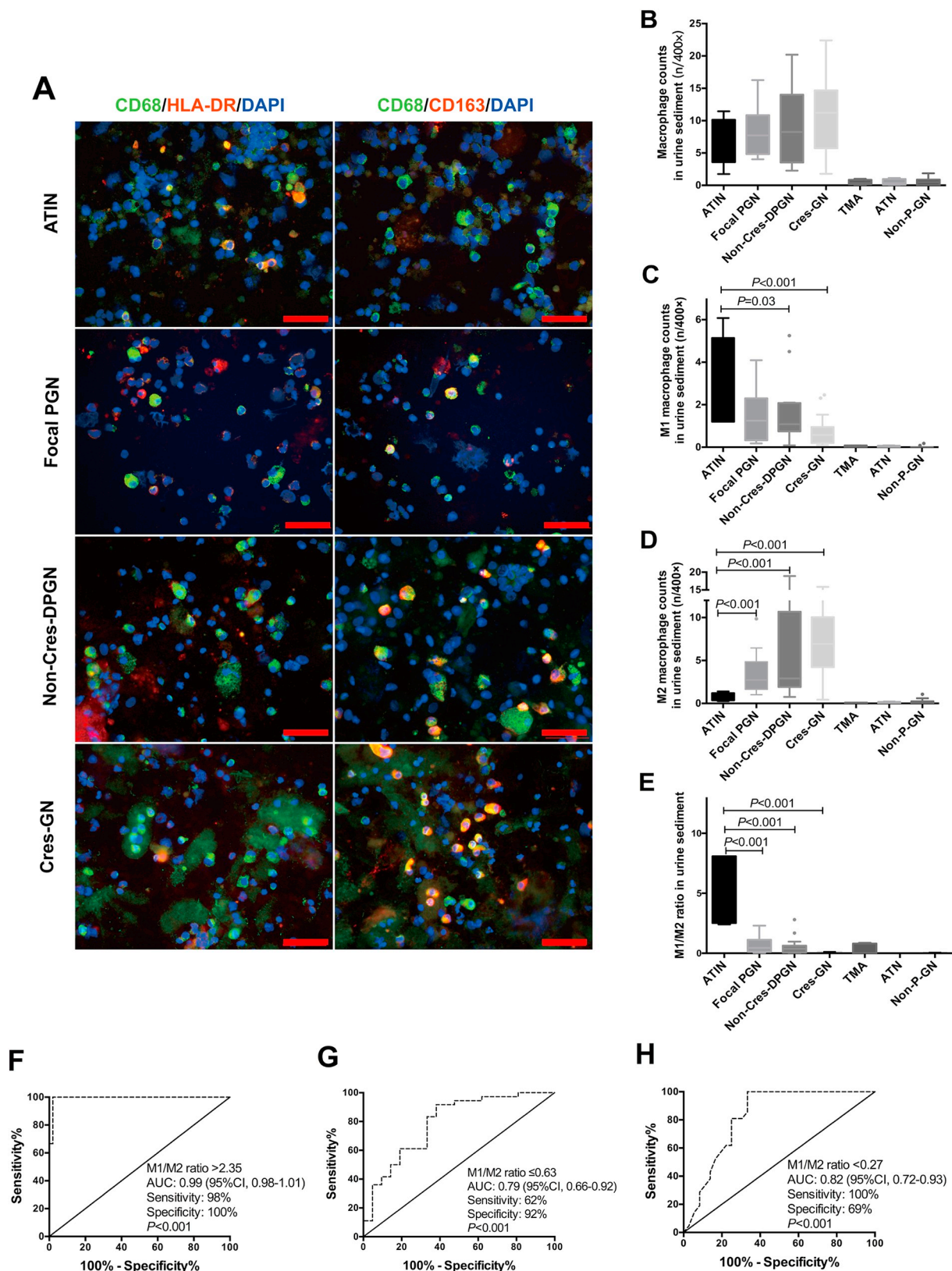
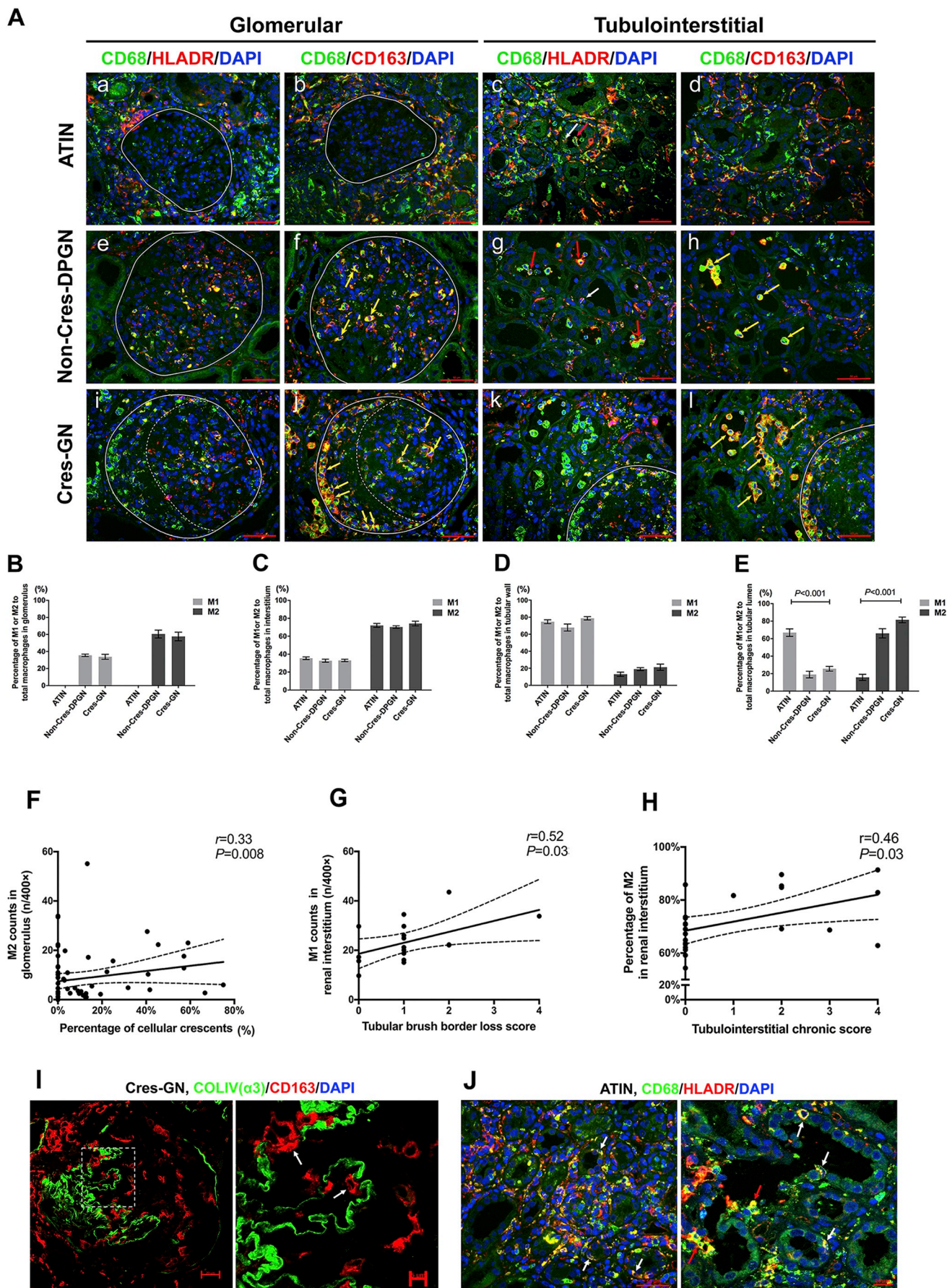


Fig. 3. Urine sediment macrophage subtypes in different groups of patients and the diagnostic significance. (A) Representative images of urine sediment co-stained with anti-CD68 (Green) and anti-HLA-DR (Red) (Left panels, M1 macrophage (yellow)), or with anti-CD68 (Green) and anti-CD163 (Red) (Right panels, M2 macrophage (yellow)) antibodies. Scale bars = 50 μ m. (B–E) Comparison of total macrophage counts (CD68 + /HLA-DR + cells) (B), M1 macrophage counts (CD68 + /HLA-DR + cells) (C), M2 macrophage counts (CD68 + /CD163 + cells) (D), and M1/M2 ratio (E) in urine sediment among different patient groups. (F–H) ROC curves depicting the ability of M1/M2 ratio to predict ATIN (F), DPGN (G) and Cres-GN (H). Values are presented as median (interquartile range); $P < .05$ was considered statistically significant. There were very few macrophages in the urine sediment from patients with TMA, ATN, or Non-P-GN, and therefore Figs. (B–E) only present the P values of comparisons among groups of ATIN, Focal-PGN, Non-Cres-DPGN and Cres-GN. (For interpretation of the references to colour in this figure legend, the reader is referred to the web version of this article.)



(caption on next page)

Fig. 4. Macrophage subtypes in renal biopsies and pathological relevance of renal macrophage polarization. (A) Representative images of renal biopsied specimens co-stained with anti-CD68 (Green) and anti-HLA-DR (Red) (M1 macrophage) or anti-CD163 (Red) (M2 macrophage) antibodies. Scale bars = 50 μ m. Glomeruli are outlined with full lines and crescents are marked with dotted lines. White arrows point at M1 macrophages infiltrating in the tubule wall and the red arrows point at M1 macrophages inside the tubular lumen (c, g) in ATIN and Non-Cres-DPGN. Yellow arrows point at M2 macrophages in the glomeruli and cellular crescents (f, j) and inside the tubular lumen (h, l) of Non-Cres-DPGN and Cres-GN. (B-E) Comparisons of M1 or M2 subtype percentage to the total macrophages counts in the compartments of glomerulus (B), interstitium (C), tubular wall (D), and tubular lumen (E) among different patient groups. Values are presented as the mean \pm SEM; $P < .05$ was considered statistically significant. (F) Correlation of M2 macrophage counts in glomerulus to the proportion of cellular crescents formation in Cres-GN. (G) Correlation of M1 macrophage in interstitium counts to tubular injury acute score in ATIN. (H) Correlation of M2 macrophage percentage in interstitium to tubulointerstitial chronic score in ATIN. (I) Co-staining of anti-CD163 (Red) and anti-COL-IV(α 3) (Green) antibodies in Cres-GN. Left panel presents a glomerulus with cellular crescent formation and broken Bowman's capsule. Right panel is the higher magnification of the outlined area. White arrows point at the CD163 + M2 macrophages (Red) breaking through the ruptured glomerular basement membrane (Green). (J) Co-staining of anti-CD68 (Green) and anti-HLA-DR (Red) antibodies in ATIN. M1 macrophages penetrate into the tubule wall (White arrows) and cross into the tubular lumen through the breaking tubule structure (Red arrows). (For interpretation of the references to colour in this figure legend, the reader is referred to the web version of this article.)

assess the relationships among u-sCD163, urine macrophage subtypes and renal infiltrated macrophage subtypes (Fig. 4A).

We found that macrophage subtypes varied according to different renal tissue compartments as well as to different disease groups. In the glomeruli, M2 macrophage predominated in DPGN, including both non-Cres-DPGN (60.5%) and Cres-GN (57.6%); no macrophages were observed in ATIN (Fig. 4A and B). In the interstitial compartment, M2 was the main subtype of macrophage both in DPGN (72.3%) and in ATIN (72.1%) (Fig. 4C). However, the mainly infiltrated macrophage subtype in the tubule wall was M1 in both ATIN (74.7%) and DPGN (73.3%) (Fig. 4D). A significant difference in the infiltrated macrophage subtype was found in the tubular lumens, with an M2 predominance in DPGN (73.8%) and M1 predominance in ATIN (66.9%) (Fig. 4E), which resulted in a marked discrepancy of M1/M2 ratio between the two disease conditions (ATIN, median 3.4, range 1.7–4.6; DPGN, median 0.27, range 0.14–0.51) ($P < .001$).

By Spearman correlation analysis, u-sCD163 levels positively correlated with the numbers of glomerular infiltrated M2 macrophage ($r = 0.61$, $P < .001$) and urine sediment M2 macrophage ($r = 0.55$, $P < .001$). Urine M2 macrophages positively correlated with glomerular infiltrated M2 macrophages ($r = 0.88$, $P < .001$), while urine M1 macrophages correlated with interstitium infiltrated M1 macrophages ($r = 0.63$, $P = .009$). This finding indicated that urine sCD163 levels and the urine M2 subtype can suggest infiltrated M2 macrophages in glomeruli, whereas the urine M1 subtype can suggest infiltrated M1 macrophage in interstitium.

3.6. Renal macrophage polarization is relevant to tissue injury

We next investigated the association of macrophage polarization in different renal compartments to the severity of tissue injury. In Cres-GN, M2 macrophages, but not M1 macrophages, predominated in the glomeruli and significantly correlated to the proportion of cellular crescents formation ($r = 0.33$, $P = .008$, Fig. 4F). By immunofluorescent staining, M2 macrophages could be detected breaking through the glomerular basement membrane (GBM) into the Bowman's capsule (Fig. 4I), which indicated a disruptive force of M2 macrophages in severe glomerulonephritis.

In the tubulointerstitial compartment, in both ATIN or Cres-GN, M1 macrophages were the leading subtype that infiltrated the tubule wall and contributed to the tubule disruption (Fig. 4J). In ATIN, tubulointerstitial M1 macrophages correlated to tubular injury acute scores ($r = 0.52$, $P = .03$), whereas the M2 subtype was associated with tubulointerstitial chronic scores ($r = 0.46$, $P = .03$) (Fig. 4G-H). These data indicated that M1 macrophages played critical roles in the acute tubular injury, while the M2 subtype might contribute to renal fibrosis in ATIN.

4. Discussion

In the present study, we investigated associations between urinary macrophage polarization markers and different causes of human

intrinsic AKI. These included urinary sCD163 (specific to M2 macrophage), urine sediment macrophage counts and subtype proportions, and pathological quantification and localization of macrophage in the kidney. In terms of diagnostic efficacy, we also compared u-sCD163 with previously well-recognized biomarkers of AKI including NGAL and KIM-1, as well as other urine macrophage markers (CD68 and CD11b). Our study revealed that assessing urine macrophage polarization could serve as valuable biomarkers for identifying the type, intensity, and location of kidney injury. All the markers of macrophage could differentiate DPGN but u-sCD163 showed better performance, and only u-sCD163 could differentiate ATN/ATIN. Thus, macrophage polarization biomarkers could provide informative insight into the complex and heterogeneous molecular mechanisms of various intrinsic AKI.

Our study showed that urinary sCD163 levels were significantly elevated in diffuse proliferative nephritis compared to focal proliferative nephritis, nonproliferative nephropathy (MCD, MN, and DN), and nonglomerular acute lesions (ATN, ATIN and TMA). U-sCD163 was also correlated with the severity and activity of glomerular injury represented by the values of serum creatinine, proteinuria, cellular crescents, and glomerular M2 macrophage infiltrates. ROC curves indicated that AUC is 0.88 for u-sCD163 > 120.3 pg/ μ mol to diagnose diffuse proliferative nephritis and 0.78 for u-sCD163 > 371.9 pg/ μ mol to diagnose cellular crescentic nephritis. These findings reinforce the role of u-sCD163 levels in predicting inflammation and glomerular injury in AASV, LN, and MPGN that have been reported recently by other groups and expand its value in distinguishing intrinsic AKI of glomerular origin from those of nonglomerular AKI [20–24,28]. Due to the lack of blood samples in our cohort, we did not analyze serum sCD163 and therefore could not correlate the levels of serum and urine sCD163 in our patients, yet it has been reported that there was no correlation between serum sCD163 and urine sCD163 in patients with ANCA-associated vasculitis [22]. And it was reported that induction therapy at the time of sampling and maintenance treatment did not influence u-sCD163 levels [24]. One strength of the current study was that we compared the diagnostic efficiency of u-sCD163 and other reported biomarkers in AKI and DPGN. Our receiver-operating characteristic curve analysis demonstrated that u-sCD163 was superior to u-CD11b and u-CD68 for the differentiation of DPGN and ATN/ATIN.

In our patient settings, it was observed that M2 macrophages predominated in the compartments of glomeruli, Bowman's capsule, and tubular lumen in proliferative nephritis, which was in line with a urine sediment M2 macrophage predominance. In contrast, in ATIN, most of the macrophages in urine sediments were the M1 subtype, which was consistent with the M1 macrophages infiltrating the tubule wall and presenting inside the tubular lumen. It is thus can be speculated that in proliferative nephritis, especially in crescentic nephritis, glomerular infiltrated M2 macrophage migrates through the destroyed capillary loop and presents in the tubular lumen, whereas in ATIN, the more invasive M1 macrophages directly infiltrate the tubular wall and go through into the tubular lumen (Fig. 5). This discrepancy in macrophage polarization between glomerular and interstitial inflammation results in a significant difference in urine sediment macrophage subtype

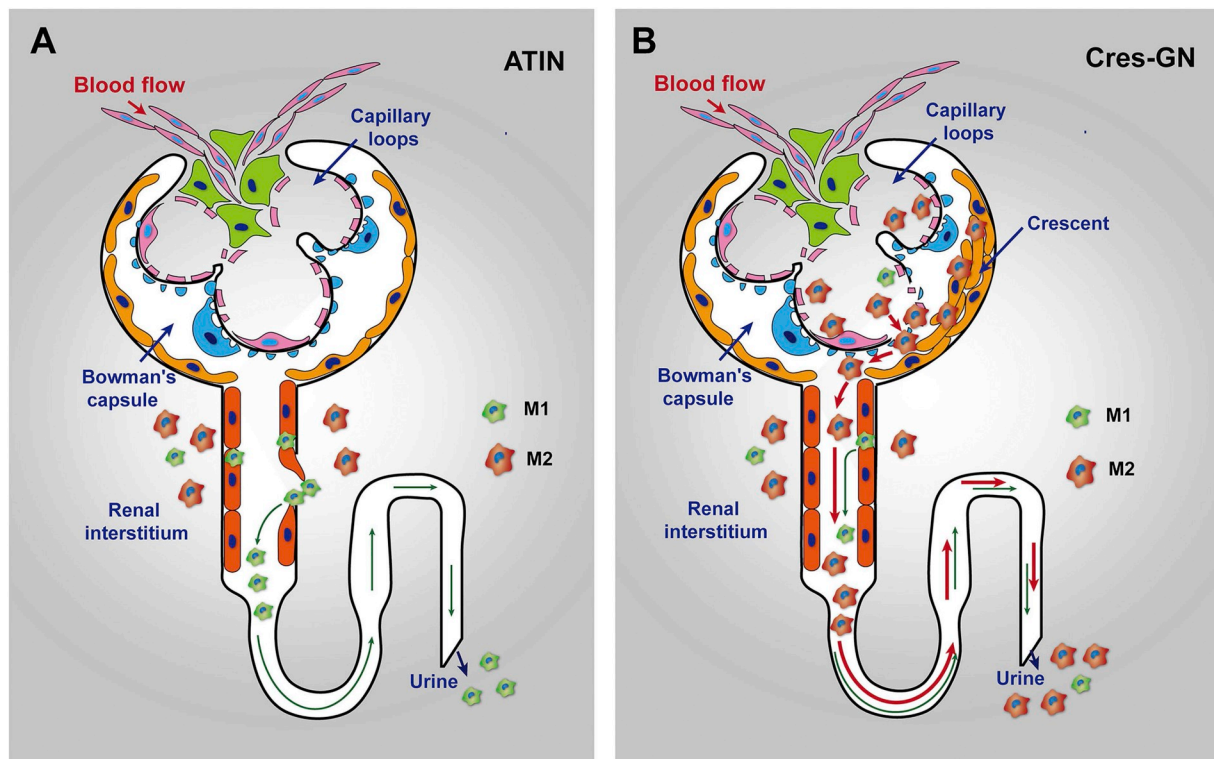


Fig. 5. Proposed model of macrophage polarization in ATIN and Cres-GN. (A) In ATIN, the glomerulus is kept intact. Although both M1 and M2 macrophages are prevalent in the interstitial area, primarily M1 macrophages infiltrate and break through the renal tubule wall and therefore results in a M1 subtype predominance in the tubular lumen and in the urine sediment. (B) In Cres-GN, M2 macrophages predominate in the glomerulus, break through the capillary wall, contribute to crescent formation, and take the majority of macrophages in the tubular lumen and in the urine sediments.

composition, which therefore could effectively help identify the location of kidney inflammatory injury. In this way, an M1 predominance in the patients' urine sediment ($M1/M2 > 2.35$) highly suggests ATIN-induced intrinsic AKI with a sensitivity of 98% and specificity of 100%, while when M2 dominates in the urine sediment ($M1/M2 < 0.27$), crescentic nephritis should be considered (sensitivity of 100% and specificity of 69%). This could be particularly meaningful when a patient with underlying CKD, for example, IgA nephropathy, develops acute renal function decline. Noninvasive urine macrophage polarization biomarkers could, therefore, help define whether the AKI was due to crescents formation or from tubulointerstitial nephritis caused by various medications.

In vitro-based M1/M2 macrophage subtypes have been increasingly linked to renal injury and repair; however, the contribution of in vivo macrophage plasticity to human kidney injury is poorly understood [19]. Although $CD163+$ M2 macrophages were found to be the major subtype of macrophages in both glomerular and interstitial compartments of PGN and in the interstitium of ATIN, the pathological relevance of these macrophages seemed to be different in various conditions. In the light of reported evidence including ours [21–24,29–31], $CD163+$ M2 macrophages correlate with the severity of glomerular destruction, indicating their potential role in facilitating acute inflammatory damage of glomeruli. While in the interstitial compartment, $HLA-DR+$ M1 macrophages correlate with the severity of acute tubulointerstitial injury, tubulitis, and renal tubular dysfunction, $CD163+$ M2 macrophage tended to be more relevant to interstitial fibrosis. These results suggest that M1 macrophages might be active mediators in human acute tubulointerstitial injury, while M2 macrophages might contribute to repair and fibrosis in the interstitial compartment.

5. Conclusions

In conclusion, our findings not only provide biomarkers that could help differentiate the type, intensity, and location of kidney injury, which may help guide clinical interventions, but also identify phenotypic and functional characteristics of macrophages in response to various stimuli in the local microenvironments of kidney injuries. Further understanding alterations of kidney microenvironment and the factors that control the phenotypes and functions of macrophages may offer an avenue for the development of new cellular and cytokine/growth factor-based therapies as alternative treatment options for patients with kidney disease.

Declaration of competing interests

None declared.

Funding

This study was supported by grants from the National Natural Science Foundation of China (No.91742205 and No.81625004) and the National Science and Technology Major Projects for “Major New Drugs Innovation and Development” of China (No. 2017ZX09304028) and Peking University Clinical Scientist Program (BMU2019LCKXJ002).

Acknowledgements

We thank the patient for devotion.

Appendix A. Supplementary data

Supplementary data to this article can be found online at <https://doi.org/10.1016/j.clim.2019.06.005>.

References

- [1] R.L. Mehta, E.A. Burdmann, J. Cerda, J. Feehally, F. Finkelstein, G. Garcia-Garcia, et al., Recognition and management of acute kidney injury in the International Society of Nephrology Oby25 Global Snapshot: a multinational cross-sectional study, *Lancet*. 387 (2016) 2017–2025.
- [2] L. Yang, G. Xing, L. Wang, Y. Wu, S. Li, G. Xu, et al., Acute kidney injury in China: a cross-sectional survey, *Lancet*. 386 (2015) 1465–1471.
- [3] R.L. Mehta, J. Cerda, E.A. Burdmann, M. Tonelli, G. Garcia-Garcia, V. Jha, et al., International Society of Nephrology's Oby25 initiative for acute kidney injury (zero preventable deaths by 2025): a human rights case for nephrology, *Lancet*. 385 (2015) 2616–2643.
- [4] L. Yang, Acute kidney injury in Asia, *Kidney Dis. (Basel)* 2 (2016) 95–102.
- [5] P.T. Murray, R.L. Mehta, A. Shaw, C. Ronco, Z. Endre, J.A. Kellum, et al., Potential use of biomarkers in acute kidney injury: report and summary of recommendations from the 10th Acute Dialysis Quality Initiative consensus conference, *Kidney Int.* 85 (2014) 513–521.
- [6] J.L. Alge, J.M. Arthur, Biomarkers of AKI: a review of mechanistic relevance and potential therapeutic implications, *Clin. J. Am. Soc. Nephrol.* 10 (2015) 147–155.
- [7] R. Chu, C. Li, S. Wang, W. Zou, G. Liu, L. Yang, Assessment of KDIGO definitions in patients with histopathologic evidence of acute renal disease, *Clin. J. Am. Soc. Nephrol.* 9 (2014) 1175–1182.
- [8] M.D. Okusa, B.L. Jaber, P. Doran, J. Duranteau, L. Yang, P.T. Murray, et al., Physiological biomarkers of acute kidney injury: a conceptual approach to improving outcomes, *Contrib. Nephrol.* 182 (2013) 65–81.
- [9] H. Rabb, M.D. Griffin, D.B. McKay, S. Swaminathan, P. Pickkers, M.H. Rosner, et al., Acute Dialysis quality initiative consensus XIII work group: inflammation in AKI: current understanding, key questions, and knowledge gaps, *J. Am. Soc. Nephrol.* 27 (2015) 371–379.
- [10] A. Zuk, J.V. Bonventre, Acute kidney injury, *Annu. Rev. Med.* 67 (2016) 293–307.
- [11] L. Yang, C.R. Brooks, S. Xiao, V. Sabbiseti, M.Y. Yeung, L.L. Hsiao, et al., KIM-1-mediated phagocytosis reduces acute injury to the kidney, *J. Clin. Invest.* 125 (2015) 1620–1636.
- [12] C. Cavanaugh, M.A. Perazella, Urine sediment examination in the diagnosis and management of kidney disease: core curriculum 2019, *Am. J. Kidney Dis.* 73 (2018) 258–272.
- [13] K. Doi, O. Nishida, T. Shigematsu, T. Sadahiro, N. Itami, K. Iseki, et al., Japanese clinical practice guideline for acute kidney injury 2016 committee: the Japanese clinical practice guideline for acute kidney injury 2016, *Clin. Exp. Nephrol.* 22 (2018) 985–1045.
- [14] H.I. Han, L.B. Skvarca, E.B. Espiritu, A.J. Davidson, N.A. Hukriede, The role of macrophages during acute kidney injury: destruction and repair, *Pediatr. Nephrol.* 34 (4) (2019) 561–569.
- [15] S.C. Huen, L.G. Cantley, Macrophages in renal injury and repair, *Annu. Rev. Physiol.* 79 (2017) 449–469.
- [16] H.R. Jang, H. Rabb, Immune cells in experimental acute kidney injury, *Nat. Rev. Nephrol.* 11 (2015) 88–101.
- [17] M. Lech, R. Grobmayr, M. Ryu, G. Lorenz, I. Hartter, S.R. Mulay, et al., Macrophage phenotype controls long-term AKI outcomes—kidney regeneration versus atrophy, *J. Am. Soc. Nephrol.* 25 (2014) 292–304.
- [18] K. Singbartl, C.L. Formeche, J.A. Kellum, Kidney-immune system crosstalk in AKI, *Semin. Nephrol.* 39 (2019) 96–106.
- [19] S. Kumar, Cellular and molecular pathways of renal repair after acute kidney injury, *Kidney Int.* 93 (2018) 27–40.
- [20] G. Olmes, M. Buttner-Herold, F. Ferrazzi, L. Distel, K. Amann, C. Daniel, CD163+ M2c-like macrophages predominate in renal biopsies from patients with lupus nephritis, *Arthritis Res. Ther.* 18 (2016) 90.
- [21] N. Endo, N. Tsuboi, K. Furuhashi, Y. Shi, Q. Du, T. Abe, et al., Urinary soluble CD163 level reflects glomerular inflammation in human lupus nephritis, *Nephrol. Dial. Transplant.* 31 (2016) 2023–2033.
- [22] V.P. O'Reilly, L. Wong, C. Kennedy, L.A. Elliot, S. O'Meachair, A.M. Coughlan, et al., Urinary soluble CD163 in active renal vasculitis, *J. Am. Soc. Nephrol.* 27 (2016) 2906–2916.
- [23] Y. Oishi, I. Manabe, Macrophages in inflammation, repair and regeneration, *Int. Immunol.* 30 (2018) 511–528.
- [24] G.J. Dekkema, W.H. Abdulahad, T. Bijma, S.M. Moran, L. Ryan, M.A. Little, et al., Urinary and serum soluble CD25 complements urinary soluble CD163 to detect active renal anti-neutrophil cytoplasmic autoantibody-associated vasculitis: a cohort study, *Nephrol. Dial. Transplant.* 34 (2019) 234–242.
- [25] A. Kitagawa, N. Tsuboi, Y. Yokoe, T. Katsuno, H. Ikeuchi, H. Kajiyama, et al., Urinary levels of the leukocyte surface molecule CD11b associate with glomerular inflammation in lupus nephritis, *Kidney Int.* 95 (2019) 680–692.
- [26] Kidney Disease, Improving global outcomes (KDIGO) acute kidney injury work group. KDIGO clinical practice guideline for acute kidney injury, *Kidney Int. Suppl.* 2 (2012) 1–138.
- [27] L.S. Chawla, R. Bellomo, A. Bihorac, S.L. Goldstein, E.D. Siew, S.M. Bagshaw, et al., Acute kidney disease and renal recovery: consensus report of the acute disease quality initiative (ADQI) 16 workgroup, *Nat. Rev. Nephrol.* 13 (2017) 241–257.
- [28] S.M. Moran, P.A. Monach, L. Zgaga, D. Cuthbertson, S. Carette, N.A. Khalidi, et al., Urinary soluble CD163 and monocyte chemoattractant protein-1 in the identification of subtle renal flare in anti-neutrophil cytoplasmic antibody-associated vasculitis, *Nephrol. Dial. Transplant.* (2018), <https://doi.org/10.1093/ndt/gfy300>.
- [29] X. Li, G. Mu, C. Song, L. Zhou, L. He, Q. Jin, et al., Role of M2 macrophages in sepsis-induced acute kidney injury, *Shock.* 50 (2) (2018) 233–239.
- [30] F. Tsai, H. Perlman, C.M. Cuda, The contribution of the programmed cell death machinery in innate immune cells to lupus nephritis, *Clin. Immunol.* 185 (2017) 74–85.
- [31] S.A. Chalmers, J. Wen, J. Shum, J. Doerner, L. Herlitz, C. Putterman, CSF-1R inhibition attenuates renal and neuropsychiatric disease in murine lupus, *Clin. Immunol.* 185 (2017) 100–108.